Why Clinically Used Tazobactam and Sulbactam Are Poor Inhibitors of OXA-10 β-Lactamase: Raman Crystallographic Evidence†

Monica A. Totir,‡,§ Jooyoung Cha,△ Akihiro Ishiwata,△ Benlian Wang,‡ Anjaneyulu Sheri,⊥ Vernon E. Anderson,‡ John Buynak,⊥ Shahriar Mobashery,△ and Paul R. Carey*,‡,§

Departments of Biochemistry and Chemistry, Case Western Reserve University, Cleveland, Ohio 44106, Department of Chemistry and Biochemistry, University of Notre Dame, Notre Dame, Indiana 46556, and Department of Chemistry, Southern Methodist University, Dallas, Texas 75205

Received November 28, 2007; Revised Manuscript Received January 16, 2008

ABSTRACT: The clinically used inhibitors tazobactam and sulbactam are effective in the inhibition of activity of class A β-lactamases, but not for class D β-lactamases. The two inhibitors exhibit a complex multistep profile for their chemistry of inhibition with class A β-lactamases. To compare the inhibition profiles for class A and D enzymes, the reactions were investigated within OXA-10 β-lactamase (a class D enzyme) crystals using a Raman microscope. The favored reaction pathway appears to be distinctly different from that for class A β-lactamases. In contrast to the case of class A enzymes that favor the formation of a key enamine species, the OXA-10 enzyme forms an α,β-unsaturated acrylate (acid or ester). Quantum mechanical calculations support the likely product as the adduct of Ser115 to the acrylate. Few enamine-like species are formed by sulbactam or tazobactam with this enzyme. Taken together, our results show that the facile conversion of the initial imine, formed upon acylation of the active site Ser67, to the *cis*- and/or *trans*-enamine is disfavored. Instead, there is a significant population of the imine that could either experience cross-linking to a second nucleophile (e.g., Ser115) or give rise to the α,β-unsaturated product and permanent inhibition. Alternatively, the imine can undergo hydrolysis to regenerate the catalytically active OXA-10 enzyme. This last process is the dominant one for class D β-lactamases since the enzyme is not effectively inhibited. In contrast to sulbactam and tazobactam, the reactions between oxacillin or 6α-hydroxyisopropylpenicillinate (both substrates) and OXA-10 β-lactamase appear much less complex. These compounds lead to a single acyl−enzyme species, the presence of which was confirmed by Raman and MALDI-TOF experiments.

β-Lactamase production is the most important mechanism by which Gram-negative bacteria become resistant to β-lactam antibiotics, such as penicillins and cephalosporins. Currently, four classes of β-lactamases have been described, of which classes A, C, and D are serine hydrolases that are similar to bacterial penicillin-binding proteins, from which they have evolved (*1–4*). The fourth class, class B β-lactamases, comprises metalloenzymes that use a zinc atom as a cofactor. The class A, C, and D enzymes react with mechanism-based inhibitors, such as the sulfone penems, by nucleophilic addition to the carbonyl of the β-lactam to form an acyl−enzyme complex (species **1**, Scheme 1) (*1*). Opening of the five-membered ring can also occur, leading to an imine, and subsequent tautomerization to enamine species. Alternatively, attack on the imine by a second nucleophile, the hydroxyl of a second serine residue, leads to irreversible inhibition (species **5** and **6**, Scheme 1) (*5*).

For the members of class D β-lactamases, compared to the better-studied class A enzymes, there is a paucity of structural and mechanistic information. This is a concern because the class D enzymes are occurring in clinical isolates with increasing frequency, where they are associated with drug resistance. There are several features that distinguish class A from class D β-lactamases. The class D β-lactamases are also known as oxacillinases for their ability to hydrolyze oxacillin and cloxacillin 2−4 times more rapidly than classical penicillins such as penicillin G (*6*). Also, they are characterized by the involvement of an N-carboxylated lysine in catalysis (*7, 8*) and by the presence of biphasic kinetics when the enzyme is not fully constituted in its N-carboxylated form (*6, 7*). Ser67, Lys70, Ser115, Lys205, and Gly207 are conserved among class D β-lactamases and are believed to be equivalent to Ser70, Lys73, Ser130, Lys234, and Gly236, respectively, in class A β-lactamases (*9*).

The OXA-10 β-lactamase, a class D β-lactamase, has significant hydrophobic character in the active site and a fold comparable to that of class A β-lactamases (*9, 10*). However, its omega loop is shorter, and it does not contain an acid side chain that would be the counterpart to Glu166 of class A β-lactamases, a residue critical for the deacylation step

† P.R.C. is supported by NIH Grant GM54072. S.M. is supported by NIH Grant AI33170 and J.B. by a grant from the Robert Welch Foundation (N-0871).

* To whom correspondence should be addressed: Department of Biochemistry, Case Western Reserve University, 10900 Euclid Ave., Cleveland, OH 44106. Phone: (216) 368-0031. Fax: (216) 368-3419. E-mail: prc5@case.edu.

‡ Department of Biochemistry, Case Western Reserve University.

§ Department of Chemistry, Case Western Reserve University.

△ University of Notre Dame.

⊥ Southern Methodist University.

10.1021/bi702348w CCC: $40.75
Published on Web 03/07/2008

Scheme 1: Proposed Reaction Mechanism of a Sulfone Inhibitor with the OXA-10 β-Lactamase

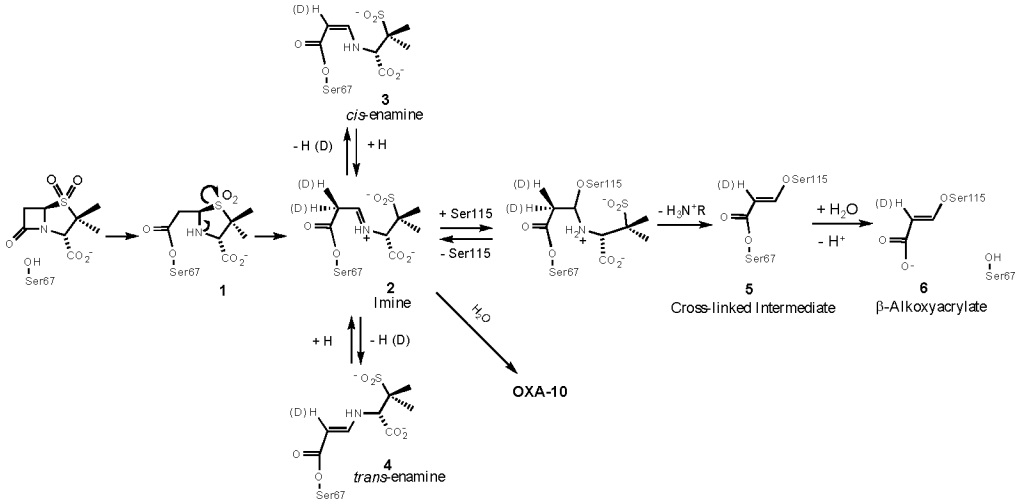

(*10*). The Ser115 side chain Oγ, corresponding to Ser130 in the class A β-lactamases, is within 3.5 Å of the Nζ and Oγ side chain atoms of Lys70 and Ser67 (*10*), a distance that would allow it to function as a second nucleophile in the OXA-10 β-lactamase (Scheme 1). The role of the second nucleophile can conceivably be assumed in the OXA-10 enzyme by the Nζ-carboxylated Lys70 residue, and it has been proposed that this residue is involved in the mechanism of action of the OXA-10 β-lactamase, having a critical role in both acylation and deacylation (*11*).

We have shown that Raman crystallography can be used to track intermediates on the reaction pathway of the deacylation deficient Glu166Ala variant of SHV-1, a class A β-lactamase, with the sulfone inhibitors tazobactam and sulbactam (*12, 13*). Crystal structures for the systems described above confirmed the formation of a *trans*-enamine intermediate, an indication that these inhibitors could follow a common pathway (*12, 14, 15*). These data will help us compare the intermediates and populations formed by the class A and class D β-lactamases with tazobactam and sulbactam and suggest a rationale for the less effective inhibition of class D enzymes by these compounds.

In this report, we present the reaction of plasmid-encoded OXA-10 β-lactamase from *Pseudomonas aeruginosa* with oxacillin, 6α-hydroxyisopropylpenicillinate, and the sulfone inhibitors tazobactam and sulbactam (Figure 1). The structure of the OXA-10 β-lactamase inhibited by 6β-hydroxyisopropylpenicillinate has been described previously and revealed

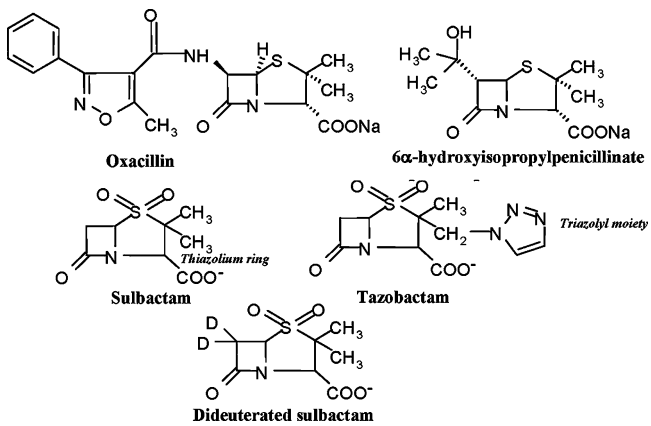

FIGURE 1: β-Lactamase substrates and inhibitors.

the formation of an acyl−enzyme complex, while the structure for the 6α-hydroxyisopropylpenicillinate complex remained elusive due to the loss of diffraction upon inhibitor "soak in" (*11*). In the work presented here, Raman crystallographic and mass spectrometric studies show the formation of an acyl−enzyme complex between the OXA-10 β-lactamase and oxacillin or 6α-hydroxyisopropylpenicillinate, following the opening of the β-lactam ring. As in the case with the SHV-1 β-lactamase, the reaction of the OXA-10 β-lactamase with the sulfone inhibitors tazobactam and sulbactam leads to the opening of the β-lactam ring, followed by the opening of the sulfone ring. For the SHV-1 intermediates, the resulting imine is converted to a fairly stable *trans*-enamine population (*12, 13*). However, for the OXA-10 reactions, little *trans*-enamine is detected. Instead, there is evidence for the formation of a population of an α,β-unsaturated acrylate or a cross-link between the α,β-unsaturated acrylate tethered to Ser67 and a second nucleophilic residue, such as species **5** and **6** in Scheme 1 (*16*). The Raman properties of these species have been characterized recently in studies involving sulbactam and 6,6-dideuterosulbactam reacting with SHV-1 β-lactamase (*16*). The facile detection of species **5** or **6** in this work with OXA-10 implies that the imine (species **2** in Scheme 1) is partitioning in that direction. An alternate fate for a fraction of the imine population is hydrolysis, and this will compete with the cross-linking pathway. The outcome of hydrolysis is regeneration of the active OXA-10 enzyme, and it is this failure to completely inhibit the enzyme that can explain the poor efficacy of sulbactam and tazobactam against class D β-lactamases.

EXPERIMENTAL PROCEDURES

Substrates and Inhibitors. Oxacillin was obtained from Sigma, and the sulfone inhibitors sulbactam (Pfizer) and tazobactam (Wyeth Pharmaceuticals) were gifts of the respective companies. The sodium salt of 6,6-(dideutero)-penicillanic acid sulfone was prepared as described in the Supporting Information of ref *16*, and 6α-hydroxyisopropylpenicillinate was prepared by the Mobashery laboratory as described in ref *17*. Stock solutions at 20 mM in 100 mM Tris (pH 8.5) were prepared to be used with the OXA-10 β-lactamase crystals.

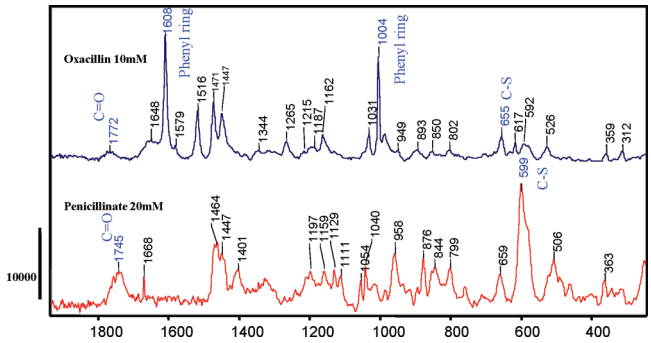

FIGURE 2: Raman spectra of oxacillin and 6α-hydroxyisopropylpenicillinate.

Protein Crystallization. The OXA-10 β-lactamase was expressed and purified as described previously (*8*). A hanging drop method was employed to obtain single crystals of the protein, as described previously (*9, 11*). In short, 1 μL of 10 mg/mL OXA-10 β-lactamase in 20 mM sodium potassium phosphate buffer (pH 7.8) was mixed at 4 °C with 1 μL of 2 M ammonium sulfate in 100 mM Tris (pH 8.5) and reservoir solution, and then the coverslip was suspended over the reservoir solution in a hanging drop configuration.

Raman Crystallography. The Raman microscope used in this study has been described previously (*18, 19*). The apoprotein crystals were removed from the mother liquor and suspended on the underside of a siliconized quartz coverslip in a 2 μL drop, containing 2 M ammonium sulfate in 100 mM Tris (pH 8.5); 120 mW of laser power, Kr^+ 647 nm, was focused using the 20× objective to a 20 μm spot size on the crystal. The crystals and the laser spot were visualized with real time color video display to ensure alignment of the crystal. The experiments were carried out at 11 °C in an ammonium sulfate solution to avoid the dissolution of the crystal. To achieve this, the crystal was set up on a coverslip resting on a metal chamber that was connected to a low-temperature thermostatically controlled bath containing a 1:1 mixture of water and glycerin. During data collection, spectra were acquired over 10 s intervals and 10 spectra were averaged for each acquisition time point. After the Raman spectrum of the apo-β-lactamase protein crystal had been recorded, 2 μL of the stock solution for an inhibitor or substrate was added to the drop to achieve a final drop volume of 4 μL and a final inhibitor or substrate concentration of 10 mM. The reaction of the inhibitor or substrate inside the OXA-10 β-lactamase was monitored as a function of time. Data collection and subtractions to obtain Raman difference spectra were performed as previously described using HoloGRAMS and GRAMS/AI 7 (ThermoGalactic, Inc., Salem, NH). The intensities of the Raman spectra were normalized to the intensity of the amide I, present at 1655 cm^{-1} in the apoenzyme spectrum, to enable the comparison of different data sets (*12*). Raman spectra of the inhibitors or substrate used were obtained under similar conditions. Spectra of 4 μL drops of inhibitor solutions prepared in 100 mM Tris buffer (pH 8.5) were obtained.

Calculations. Ab initio quantum mechanical calculations were performed to predict the Raman spectra of model intermediate compounds using Gaussian 03 (*20*). Calculations were performed at the Hartree–Fock and DFT B3LYP levels using a 6-31G+d basis set.

Mass Spectrometry. Oxacillin was dissolved in 25 mM HEPES buffer and mixed with the OXA-10 β-lactamase in a molar ratio of 11000:1 (substrate:enzyme) at room temperature for 70 min. The apoprotein and the OXA-10 β-lactamase complexed with oxacillin were denatured with 8 M urea at 50 °C for 30 min, similar to the procedure of Pagan-Rodriguez et al. (*21*). The pH was adjusted to 8 using 0.4 M NH_4HCO_3, and after a 1:5 dilution of the mixture with water, trypsin was added at a 1:30 (w/w) ratio. The final mixture was incubated at 37 °C for 12 h, then frozen, and stored at −80 °C. The digestion products were analyzed using matrix-assisted laser desorption ionization time-of-flight (MALDI-TOF)[1] mass spectrometry. The data were acquired in reflectron and positive ion mode on a Bruker BiFlex III instrument equipped with a pulsed nitrogen laser (377 nm) and an accelerating voltage of 20 kV. The matrix, α-cyano-4-hydroxycinnamic acid, was prepared fresh daily as a solution mixture containing acetonitrile and 0.1% trifluoroacetic acid (70:30). After thawing, the tryptic digestion peptides were desalted using micro Zip Tips C18 (Millipore), according to the manufacturer's directions, being eluted directly onto the stainless steel MALDI plate. The spectra were mass calibrated using five tryptic peptides from OXA-10, *m/z* range from 950.40 to 1499.67.

RESULTS AND DISCUSSION

Oxacillin and 6α-Hydroxyisopropylpenicillinate React with OXA-10 β-Lactamase To Form Acyl−Enzyme Species. Figure 2 shows the Raman difference spectra, with the spectra of the solvents subtracted, of oxacillin and 6α-hydroxyisopropylpenicillinate by themselves. Key features due to the carbonyl stretch of the β-lactam ring and the C−S stretch from the thiazolidine ring are identified in the spectra. For oxacillin, the lactam carbonyl Raman peak occurs at 1772 cm^{-1} and a C−S stretch from the thiazolidine ring appears at 655 cm^{-1}, while for 6α-hydroxyisopropylpenicillinate, the carbonyl Raman peak is at 1745 cm^{-1} and a C−S stretch appears at 599 cm^{-1}. The apparent difference in the positions of the C−S modes is due to vibrational coupling; in both spectra, bands near 595 and 655 cm^{-1} contain significant C−S stretch character. Although the lactam carbonyls for the two compounds appear at different positions, they fall within the accepted range, 1730–1780 cm^{-1}, for four-member ring lactams. The C═O and C−S peaks were used to monitor the integrity of the rings as the compounds were infused into the OXA-10 β-lactamase crystals. Raman difference spectra resulting from oxacillin (blue) and 6α-hydroxyisopropylpenicillinate (red) soaked into the OXA-10 β-lactamase are shown in Figure 3. Figure 3A, depicting oxacillin reacting inside an OXA-10 β-lactamase crystal, shows no evidence of the β-lactam carbonyl stretch near 1772 cm^{-1}, indicating that the β-lactam ring has opened. The lower trace of penicillinate reacting with OXA-10 shows traces of the C═O stretch near 1745 cm^{-1}, which indicates that a certain amount of the penicillinate compound remained intact and is likely bound in the crystal in a nonspecific manner. If we take the 1465 and 1448 cm^{-1} features in Figures 2 and 3A, due to C−H motions, as internal standards, we can use the intensity

[1] Abbreviations: MALDI-TOF, matrix-assisted laser desorption ionization time-of-flight; DFT, density functional theory.

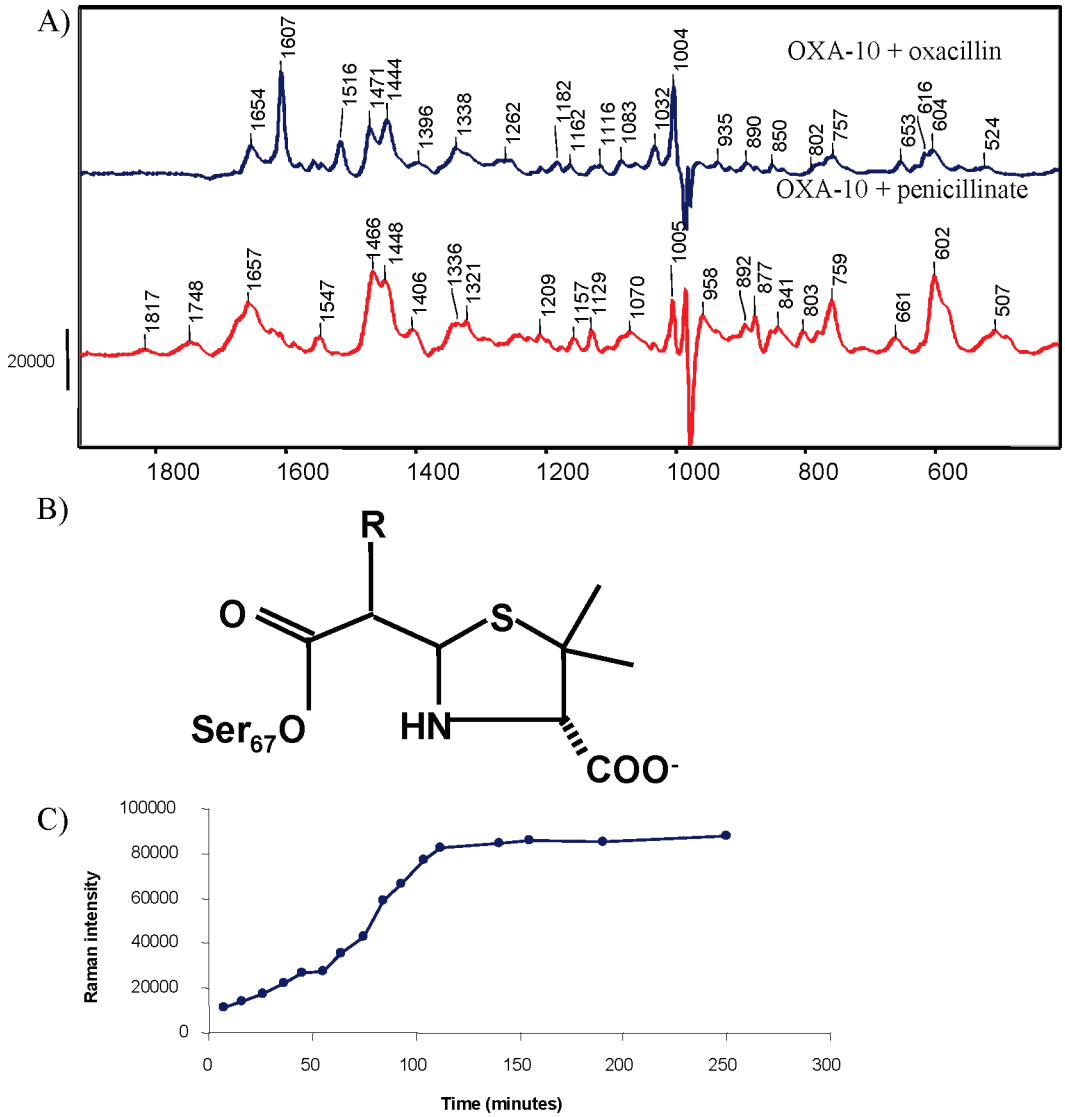

FIGURE 3: (A) Raman difference spectra of the OXA-10 β-lactamase crystal with oxacillin (45 min soak, blue) and 6α-hydroxyisopropylpenicillinate (62 min soak, red) soaked in, where the vertical bar represents a 20000-photon event. (B) Chemical structure of the acyl−enzyme complex formed by the OXA-10 β-lactamase with oxacillin and 6α-hydroxyisopropylpenicillinate. (C) Time dependence of the 1607 cm^{-1} peak given by oxacillin diffusing into the OXA-10 β-lactamase crystal.

of the 1748 cm^{-1} feature to estimate that 50% of the penicillinate is nonspecifically bound. The data in Figure 3A were recorded in the 45–60 min "soak in" time frame, during which both compounds give an acyl−enzyme complex. The most direct spectroscopic evidence for this would be an ester C═O feature in the 1710–1740 cm^{-1} region due to acylation at Ser67. However, features in this region cannot be identified with certainty in the difference spectrum due to the difficulties of obtaining accurate spectral subtractions in the amide I region, 1610−1710 cm^{-1}. Instead, we are able to characterize other bands that can be assigned to the acyl−enzyme complex. The basis for this is the comparison between the experimental data (Figure 3A) and Gaussian-based quantum mechanical calculations carried out on the fragment shown in Figure 3B, where Ser67 and R were replaced with methyl groups. Key results from the quantum chemical calculations are given in Table 1 and allow us to assign many of the features in Figure 3A. The C_3 carboxylate symmetric stretch at 1374 cm^{-1} in the calculated spectrum corresponds to the broad 1396 cm^{-1} (oxacillin) or 1406 cm^{-1} (penicillinate) peak in the experimental data. The feature near 1330 cm^{-1} in the experimental data corresponds to the 1291 cm^{-1} feature in Table 1 and is evidence that the thiazolidine ring is still intact, since this vibrational mode is assigned to the ring thiazolidine breathing modes coupled with the C_3 carboxylate stretching motion. Another indication that the thiazolidine ring is intact is the presence in the experimental data of the C−N stretch ring mode at 1116 cm^{-1} for oxacillin or at 1129

Table 1: Most Intense Calculated Raman Vibrational Modes and Their Assignment for the Acyl−Enzyme Complex Shown in Figure 3B, where R and Ser_{67} Were Replaced with Methyl Groups

experimental/*calculated* Raman ν (cm^{-1}) for the acyl−enzyme complex (intensities in parentheses)	assignment
1396 (oxacillin), **1406** (penicillinate)/*1374 (8)*	C_3, COO^- symmetric stretch, ring breathing, NH wagging
1330 (oxacillin and penicillinate)/*1291 (9)*	ring breathing, C_3, COO^- symmetric stretch
1116 (oxacillin), **1129** (penicillinate)/*1105 (5)*	C−N ring stretch, C−H rocking
890, **850**, **802** (oxacillin), **877**, **841**, **803** (penicillinate)/*815 (9)*, *791 (5)*, *772 (7)*	ring breathing, delocalized modes

cm^{-1} for hydroxyisopropylpenicillinate, which correlates with the feature at 1105 cm^{-1} in the calculated results (Table 1). In these comparisons, the agreement between experimental and calculated frequencies is seldom exact, reflecting the approximations inherent to the calculations. The lower-wavenumber features seen below 970 cm^{-1} are given by the thiazolidine ring breathing and delocalized modes. It is remarkable that both of the compounds give a similar triad of features in the acyl−enzyme complex at 890, 850, and 802 cm^{-1} for oxacillin and at 892, 841, and 803 cm^{-1} for 6α-hydroxyisopropylpenicillinate. Although, again, the correspondence is not exact, features in this region are reproduced in the calculations and are assigned to ring breathing modes (Table 1). The lower-wavenumber region for the oxacillin-based acyl−enzyme complex (Figure 3A) shows the thiazolidine C−S stretch ring mode at 655 cm^{-1} and at 599 cm^{-1} for penicillinate, providing further evidence that the five-membered rings remain intact. For the oxacillin-based acyl−enzyme complex, the presence of ring modes at 1607, 1516, and 1444 cm^{-1} from the phenyl and the thiazolidine moieties demonstrates that these functionalities are retained in the acyl−enzyme complex. For oxacillin, the time dependence of the ligand penetration and acylation in the crystal can be measured by the rise of the 1607 cm^{-1} feature, due to the phenyl group of oxacillin. The process is slow, reaching a maximum constant value at 100 min (Figure 3C). This can be explained, in part, by a slow diffusion of oxacillin within the crystal due to its larger side chain, compared to 6α-hydroxyisopropylpenicillinate and the sulfone inhibitors tazobactam and sulbactam. This is supported by modeling studies in which oxacillin is overlaid in the active site of the published structure for 6β-hydroxyisopropylpenicillinate in OXA-10 β-lactamase, which leads to steric clashes of the phenyl group of the oxacillin with Ser115 and Lys205 in the active site (data not shown). Thus, to be able to acylate Ser67, oxacillin must "bend" in the active site, probably stacking on top of Trp154.

The acyl−enzyme complex was observed, as well, by mass spectrometric studies using MALDI-TOF experiments for oxacillin reacting with the OXA-10 β-lactamase. The data are summarized in Figure 4, where panel A shows the tryptic peptide EYLPASTFK containing the acylating Ser67 at *m/z* 1055.52 for the trypsin-digested apo OXA-10 β-lactamase. Reacting oxacillin with the OXA-10 β-lactamase for 70 min and digesting the mixture with trypsin lead to the disappearance of the *m/z* 1055.52 peak and the appearance of the acyl−enzyme complex revealed by two peaks (Figure 4B). The prominent peak at *m/z* 1456.61 confirms the formation of a 401.105 Da adduct, indicative of the acyl−enzyme complex shown in Figure 3B. The second feature is observed at *m/z* 1478.60 and is attributed to the $-H + Na^+$ adduct of oxacillin-modified tryptic peptides.

OXA-10 β-Lactamase Reacting with Tazobactam, Sulbactam, and Dideuterated Sulbactam Forms an α,β-Unsaturated Product in Tens of Minutes. The Raman spectra of tazobactam and sulbactam in buffer have been described previously (*12*), and the spectrum of 6,6-dideuterated sulbactam is shown in the Supporting Information (Figure 1S). The Raman difference spectra, 1100–1900 cm^{-1}, of tazobactam (red), sulbactam (blue), and dideuterated sulbactam (green) infused into an OXA-10 β-lactamase crystal are presented in Figure 5. All three compounds underwent the requisite β-lactam ring opening after soaking in for 35–80 min, since the characteristic β-lactam carbonyl features, at 1780 cm^{-1} for tazobactam and at 1772 cm^{-1} for sulbactam, disappear (Figure 5) (*12*). Sulbactam and dideuterated sulbactam also display a loss of the ring C−S stretch at 635 and 616 cm^{-1} (Figure 1S of the Supporting Information), respectively, coming from the thiazol ring, indicating the opening of this ring (data not shown). For tazobactam, we observe traces of the 627 cm^{-1} C−S stretch peak still present (data not shown). The 627 cm^{-1} feature indicates that a small amount of the tazobactam did not undergo a complete rearrangement, and for this population, only the β-lactam ring is hydrolyzed, which corresponds to species **1** in Scheme 1.

In earlier studies, for sulbactam and tazobactam reacting with Glu166Ala SHV-1 β-lactamase (*12*), we observed only the formation of a *trans*-enamine population that gives rise to characteristic, intense Raman features near 1595 cm^{-1} (*12, 14*). In our study with OXA-10, the low-intensity peaks near 1600 cm^{-1} may have a contribution from an enamine or imine species. If indeed these are from enamine-like species, the low intensity suggests that the enamine must be a minor population. The predominant feature in Figure 5 is the intense broad band near 1520 cm^{-1}, which appears in minutes and increases slowly over a 100 min period. The band is identified below on the basis of calculations reported by Totir et al. (*16*). In that study, we undertook quantum chemical calculations on compounds that model species **5** and **6** in Scheme 1, where the serine side chains were replaced with methyl moieties (*16*).

The calculations showed that for the nonstrained model compounds the most intense Raman modes appear near 1565 and 1534 cm^{-1}, for the species **5** and **6** models, respectively. On this basis, species **6** in Scheme 1 is the prime candidate for the molecule giving rise to many of the features seen in the Raman difference spectra in Figure 5, with species **5** being a possible candidate if it has a conformation in the active site that is disturbed from the planar "relaxed" form used in the calculations. The assignment to species **6** is strengthened by the correspondence shown between several experimental and theoretical bands. For example, the calculated bands in Table 2 at 1424, 1332, and 1242 cm^{-1} all appear to have corresponding features in the experimental data shown in Figure 5. The identity of species **6** is further supported by the effects of isotopic substitutions. Gaussian calculations predict the main feature at 1534 cm^{-1} in the unlabeled compound ($CH_3OCHCHCOO^-$) is shifted to 1513 cm^{-1} for the intermediate resulting from the 6,6-dideuterated sulbactam [$CH_3OCHCDCOO^-$ (Table 2)]. In the experimental data (Figure 5), we can identify a similar downshift from 1522 to 1511 cm^{-1}. The only other feature that shifts in the experimental data for sulbactam vis-à-vis dideuterated sulbactam is the band at 1240 cm^{-1} that moves to 1234 cm^{-1} in the spectrum generated using 6,6-dideuterated sulbactam. This shift is reproduced well in the calculated spectrum, where the 1242 cm^{-1} feature moves to 1235 cm^{-1} (Table 2). The other main features near 1629 and 1424 cm^{-1} have the same position in the calculations for both model compounds, in agreement with the experimental data.

Figure 6 plots the time course of the increase in intensity of the peak near 1520 cm^{-1} for tazobactam, sulbactam, and 6,6-dideuterosulbactam. One can see that sulbactam forms the 1520 cm^{-1} species more readily than tazobactam, but

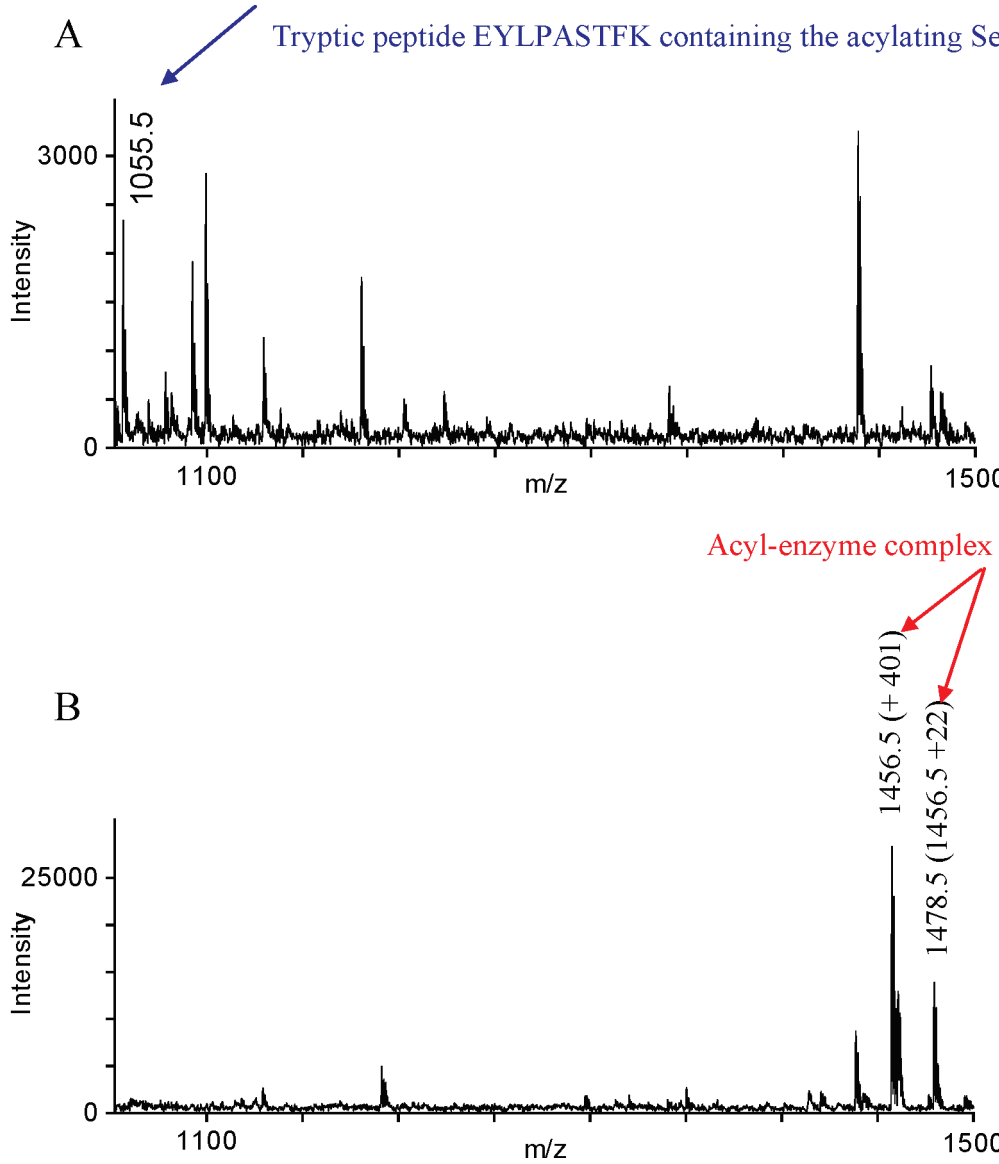

FIGURE 4: MALDI-TOF of the OXA-10 β-lactamase (A) and the OXA-10 β-lactamase with oxacillin (B). The peptide of residues 42–50 (EYLPASTFK, *m/z* 1055.5) from the OXA-10 β-lactamase disappears when the OXA-10 β-lactamase reacts with oxacillin, and a new peak at *m/z* 1456.5 is observed.

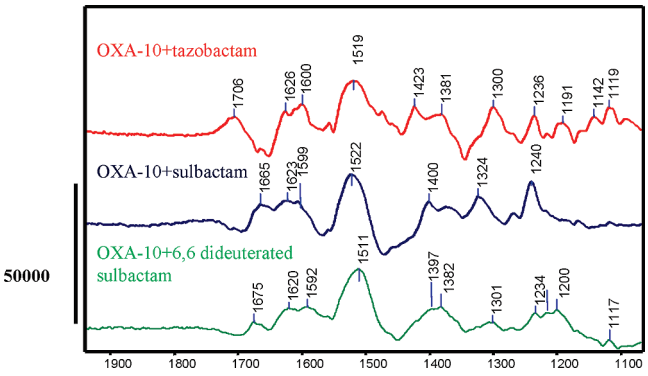

FIGURE 5: Raman difference spectra of the OXA-10 β-lactamase crystal with tazobactam (red, 84 min soak) and sulbactam (blue, 36 min soak). The vertical bar represents a 50000-photon event.

both reactions are slow with, for example, the sulbactam feature taking 40–50 min to level off. These values compare to the lifetime of a bacterium which is typically 20–30 min.

We have also taken into account the possibility of Lys70 acting as a second nucleophile (*22*) in the active site of OXA-10, leading to trans-imination of the acyl−enzyme complex and the final formation of However, Gaussian calculations

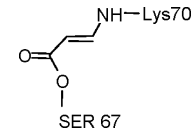

performed on a model of this species, where the serine and lysine side chains were replaced with methyl groups, showed that the most intense Raman band for this species is predicted to occur near 1630 cm^{-1} (unpublished data), which is not seen in the experimental results. This is also consistent with the side chain of Lys70 being tied up as a carbamate (N-carboxylated lysine).

Why Tazobactam and Sulbactam Are Poor Inhibitors of Class D β-Lactamases. The findings described above may now be summarized. There is clear spectroscopic evidence, principally a band near 1520 cm^{-1}, for sulbactam and tazobactam reacting with the OXA-10 β-lactamase leading to the formation of an α,β-unsaturated product on the time

Table 2: Comparison of the Main Features in Experimental Raman Spectra for Tazobactam, Sulbactam, and Dideuterated Sulbactam Reacting with the OXA-10 β-Lactamase, Correlated with the Features in the Calculated Raman Spectra Given by 3-Methoxyacrylate and Deuterated 3-Methoxyacrylate

Raman ν (cm^{-1}) for tazobactam/ sulbactam/ dideuterated sulbactam reacting with OXA-10	calculated Raman ν (cm^{-1}) for $CH_3OCHCHCOO^-$/ $CH_3OCHCDCOO^-$ (intensities in parentheses)	assignment
1626/1623/1620	1629 (37)/1627 (34)	CH wagging and COO^- antisymmetric stretching
1519/1522/1511	1534 (80)/1513 (92)	C=C, COO^- stretching, delocalized stretching over the entire chain
1423/1400/1397	1424 (8)/1423 (14)	CH wagging, COO^- stretching
1300/1324/1301	1332 (32)	CH_3, CH wagging, delocalized stretching over the entire chain
1236/1240/1234	1242 (24)/1235 (30)	CH wagging, COO^- stretching

scale of tens of minutes; this is probably species **6** in Scheme 1. In addition, there is evidence for minor populations of enamine and/or imine intermediates with both sulfone inhibitors. This is in marked contrast to the reaction with the class A SHV-1 β-lactamase, where only *trans*-enamine species are seen in the time frame of 120 min (*12*). However, for the Glu166Ala variant of SHV-1 β-lactamase, very long reaction times in the crystals, >20 h, do lead to the appearance of a 1520 cm^{-1} feature (*16*). The results for tazobactam and sulbactam reacting with the SHV-1 or OXA-10 β-lactamases, taken together, suggest why these inhibitors are less effective with the OXA-10 β-lactamase. Sulbactam and tazobactam react with both SHV-1 and OXA-10 β-lactamases to form initially imine intermediates. For SHV-1, the preferred reaction pathway is for the imine to tautomerize to form a *trans*-enamine, a fairly stable intermediate leading to effective inhibition. However, for OXA-10, at best a small population of enamine is formed from the imine. The imine itself may be present as an intermediate, but detection by our method is problematic due to its low Raman intensity. Instead, the imine undergoes a cross-linking reaction, probably involving Ser115, that leads to a 3-serine acrylate and irreversibly inhibits the enzyme. However, this reaction is slow, taking 30–50 min to reach the maximum

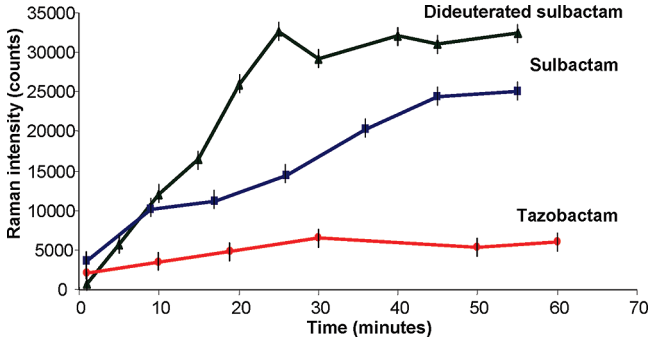

FIGURE 6: Time dependence for the Raman feature near 1520 cm^{-1} formed by tazobactam (red), sulbactam (blue), and dideuterated sulbactam (black) soaking into crystals of OXA-10 β-lactamase. The vertical lines represent the errors (standard deviations) in measuring the Raman intensity.

population giving rise to the 1520 cm^{-1} feature (Figure 6). Whereas this reaction could be observed in our experiments with rather large concentrations of the inhibitors, we propose that the situation in vivo is different in the presence of limiting concentrations of the inhibitors. We postulate that the length of time needed for the formation of the requisite species with the resonance of 1520 cm^{-1} is simply too long and that the process is not competitive. Hence, hydrolysis of imine regenerates a substantial population of active OXA-10 and renders total inhibition of the enzyme ineffective.

CONCLUSION

Imine at the Crossroads. These studies, taken with our earlier work on sulfones reacting with SHV-1 β-lactamase, emphasize the effectiveness of inhibition by sulfones depends on the fate of the imine species (species **2** in Scheme 1) formed immediately after sulfone ring opening. The imines formed by tazobactam or sulbactam reacting with SHV-1 undergo rapid tautomerization leading to the corresponding *trans*-enamines. The latter are fairly stable and effectively block the enzyme's active site. However, this reaction pathway is not favored by OXA-10, where the imine can undergo two alternate reactions. It can react with a second nucleophile leading to irreversible inhibition via cross-linking in the active site. We have characterized the product of this reaction in this work, and this occurs fairly slowly over a time course of tens of minutes in crystals of OXA-10. This exposes the imine to the competing reaction with water molecules. The resulting hydrolysis regenerates an active enzyme population, thus providing a rationale for the relative ineffectiveness of sulbactam and tazobactam against class D β-lactamases.

ACKNOWLEDGMENT

We thank Dr. Pius Padayatti for the assistance in the modeling of the oxacillin in the active site of the OXA-10 β-lactamase. We are grateful to Dr. Robert Bonomo for comments on the manuscript.

SUPPORTING INFORMATION AVAILABLE

Raman spectrum of 6,6-dideuterated sulbactam. This material is available free of charge via the Internet at http://pubs.acs.org.

REFERENCES

1. Ambler, R. P. (1980) The structure of β-lactamases. *Philos. Trans. R. Soc. London, Ser. B 289*, 321–331.
2. Bush, K. A. (2001) New β-lactamases in Gram-negative bacteria: Diversity and impact on the selection of antimicrobial therapy. *Clin. Infect. Dis. 32*, 1085–1089.
3. Medeiros, A. A. (1997) Evolution and dissemination of β-lactamases accelerated by generations of β-lactam antibiotics. *Clin. Infect. Dis. 24*, 19–45.
4. Fisher, J. F., Meroueh, S. O., and Mobashery, S. (2005) Bacterial resistance to β-lactam antibiotics: Compelling opportunism, compelling opportunity. *Chem. Rev. 105*, 395–424.
5. Kuzin, A. P., Nukaga, M., Nukaga, Y., Hujer, A. M., Bonomo, R. A., and Knox, J. R. (2001) Inhibition of the SHV-1 β-lactamase by sulfones: Crystallographic observation of two reaction intermediates with tazobactam. *Biochemistry 40*, 1861–1866.
6. Ledent, P., Raquet, X., Joris, B., Van Beeumen, J., and Frere, J. M. (1993) A comparative study of class-D β-lactamases. *Biochem. J. 292*, 555–562.

7. Golemi, D., Maveyraud, L., Vakulenko, S., Samama, J. P., and Mobashery, S. (2001) Critical involvement of a carbamylated lysine in catalytic function of class D β-lactamases. *Proc. Natl. Acad. Sci. U.S.A. 98*, 14280–14285.
8. Golemi, D., Maveyraud, L., Vakulenko, S., Tranier, S., Ishiwata, A., Kotra, L. P., Samama, J.-P., and Mobashery, S. (2000) The First Structural and Mechanistic Insights for Class D β-Lactamases: Evidence for a Novel Catalytic Process for Turnover of β-Lactam Antibiotics. *J. Am. Chem. Soc. 122*, 6132–6133.
9. Maveyraud, L., Golemi, D., Kotra, L. P., Tranier, S., Vakulenko, S., Mobashery, S., and Samama, J.-P. (2000) Insights into Class D β-Lactamases Are Revealed by the Crystal Structure of the OXA10 Enzyme from *Pseudomonas aeruginosa*. *Structure 8*, 1289–1298.
10. Paetzel, M., Danel, F., de Castro, L., Mosimann, S. C., Page, M. G. P., and Strynadka, N. C. J. (2000) Crystal structure of the class D β-lactamase OXA-10. *Nat. Struct. Biol. 7*, 918–925.
11. Maveyraud, L., Golemi-Kotra, D., Ishiwata, A., Meroueh, O., Mobashery, S., and Samama, J.-P. (2002) High-Resolution X-ray Structure of an Acyl-Enzyme Species for the Class D OXA-10 β-Lactamase. *J. Am. Chem. Soc. 124*, 2461–2465.
12. Helfand, M. S., Totir, M. A., Carey, M. P., Hujer, A. M., Bonomo, R. A., and Carey, P. R. (2003) Following the Reactions of Mechanism-Based Inhibitors with β-Lactamase by Raman Crystallography. *Biochemistry 42*, 13386–13392.
13. Totir, M. A., Padayatti, P. S., Helfand, M. S., Carey, M. P., Bonomo, R. A., Carey, P. R., and Akker, F. v. d. (2006) Effect of the Inhibitor-Resistant M69V Substitution on the Structures and Populations of trans-Enamine β-Lactamase Intermediates. *Biochemistry 45*, 11895–11904.
14. Padayatti, P. S., Helfand, M. S., Totir, M. A., Carey, M. P., Hujer, A. M., Carey, P. R., Bonomo, R. A., and Akker, F. v. d. (2004) Tazobactam Forms a Stoichiometric trans-Enamine Intermediate in the E166A Variant of SHV-1 β-Lactamase: 1.63 Å Crystal Structure. *Biochemistry 43*, 843–848.
15. Padayatti, P. S., Helfand, M. S., Totir, M. A., Carey, M. P., Carey, P. R., Bonomo, R. A., and van den Akker, F. (2005) High Resolution Crystal Structures of the trans-Enamine Intermediates Formed by Sulbactam and Clavulanic Acid and E166A SHV-1 β-Lactamase. *J. Biol. Chem. 280*, 34900–34907.
16. Totir, M. A., Helfand, M. S., Carey, M. P., Sheri, A., Buynak, J. D., Bonomo, R. A., and Carey, P. R. (2007) Sulbactam Forms Only Minimal Amounts of Irreversible Acrylate-Enzyme with SHV-1 β-Lactamase. *Biochemistry 46*, 8980–8987.
17. Mourey, L., Miyashita, K., Swarén, P., Bulychev, A., Samama, J. P., and Mobashery, S. (1998) Inhibition of the NMC-A β-lactamase by a Penicillanic Acid Derivative, and the Structural Bases for the Increase in Substrate Profile of This Antibiotic Resistance Enzyme. *J. Am. Chem. Soc. 120*, 9382–9383.
18. Altose, M. D., Zheng, Y., Dong, J., Palfey, B. A., and Carey, P. R. (2001) Comparing protein-ligand interactions in solution and single crystals by Raman spectroscopy. *Proc. Natl. Acad. Sci. U.S.A. 98*, 3006–3011.
19. Dong, J., Swift, K., Matayoshi, E., Nienaber, V. L., Weitzberg, M., Rockway, T., and Carey, P. R. (2001) Probing Inhibitors Binding to Human Urokinase Crystals by Raman Microscopy: Implications for Compound Screening. *Biochemistry 40*, 9751–9757.
20. Frisch, A., Frisch, M. J., and Trucks, G. W. (2003) *Gaussian 03*, Gausssian Inc., Wallingford, CT.
21. Pagan-Rodriguez, D., Zhou, X., Simmons, R., Bethel, C. R., Hujer, A. M., Helfand, M. S., Jin, Z., Guo, B., Anderson, V. E., Ng, L. M., and Bonomo, R. A. (2004) Tazobactam inactivation of SHV-1 and the inhibitor-resistant Ser130-Gly SHV-1 β-Lactamase: Insight into the mechanism of inhibition. *J. Biol. Chem. 279*, 19494–19501.
22. Knowles, J. R. (1985) Penicillin Resistance: The Chemistry of β-Lactamase Inhibition. *Acc. Chem. Res. 18*, 97–104.

BI702348W